

1 **Unusual subpolar North Atlantic phytoplankton bloom in 2010: volcanic**
2 **fertilisation or North Atlantic Oscillation?**

3

4 Stephanie A. Henson^{1*}, Stuart C. Painter¹, N. Penny Holliday¹, Mark C.
5 Stinchcombe¹, Sarah L. C. Giering^{2†}

6

7 ¹*National Oceanography Centre, European Way, Southampton, SO14 3ZH, UK.*

8 ²*Ocean and Earth Science, University of Southampton, Waterfront Campus,*
9 *Southampton, SO14 3ZH, UK.*

10 [†]*Now at: Oceanlab, University of Aberdeen, Newburgh, Aberdeenshire, AB41 6AA,*
11 *UK.*

12 **Corresponding author: S.Henson@noc.ac.uk*

13 **Key Points:**

14 Anomalously strong phytoplankton bloom observed in 2010 in North Atlantic

15 Volcanic eruption and North Atlantic Oscillation considered as drivers

16 Synthesis of in situ and satellite data reveals links to unusual conditions

17 **Index Terms**

18 Oceanography: General: Climate and interannual variability

19 Oceanography: General: Physical and biogeochemical interactions

20 Oceanography: Physical: Decadal ocean variability

21 Oceanography: Biological and chemical: Phytoplankton

22 **Keywords**

23 Satellite ocean colour, spring bloom, interannual variability, freshwater anomaly

24 **Running Title**

25 Unusual North Atlantic bloom

26 **Abstract**

27 In summer and autumn 2010, a highly anomalous phytoplankton bloom, with
28 chlorophyll concentration more than double that of previous years, was observed in
29 the Irminger Basin, southwest of Iceland. Two unusual events occurred during 2010
30 which had the potential to promote the unusual bloom. Firstly, in spring 2010, the
31 Eyjafjallajökull volcano in Iceland erupted, depositing large quantities of tephra into
32 the subpolar North Atlantic. Secondly, during the winter of 2009/2010 the North
33 Atlantic Oscillation (NAO) became extremely negative, developing into the second
34 strongest negative NAO on record. Hydrographic conditions were highly anomalous
35 in the region, with an influx of freshwater spreading through the basin, and unusual
36 nutrient and mixed layer depth conditions. Here we use a combination of satellite,
37 modelled and *in situ* data to investigate whether the input of iron from the volcanic
38 eruption or change in hydrographic conditions due to the extreme negative NAO were
39 responsible for the anomalous phytoplankton bloom. We conclude that changes in
40 physical forcing driven by the NAO, and not the volcanic eruption, stimulated the
41 unusual bloom.

42

43 **1. Introduction**

44 In April/May 2010, the Eyjafjallajökull volcano in Iceland erupted, disrupting
45 air travel throughout Europe and producing an estimated 270 million cubic metres of
46 airborne tephra, of which roughly half fell in Iceland, with much of the remainder
47 deposited in the surface waters of the North Atlantic [*Gudmundsson et al.*, 2012;
48 *Karlsdottir et al.*, 2012]. Because volcanic ash contains iron, an important
49 micronutrient for phytoplankton growth, eruptions are postulated to have potentially
50 large effects on oceanic primary production (PP; *Duggen et al.*, 2010). Marine
51 sediment records contain evidence of volcanic ash deposition events throughout
52 Earth's history, and results from field investigations suggest that these events may
53 have been responsible for large scale climatic changes [*Robock*, 2000]. The eruption
54 of Mt. Pinatubo in 1991, for example, coincided with a drawdown of CO₂ in the
55 Northern Hemisphere, hypothesized to be driven by increased PP stimulated by
56 natural iron fertilisation following ash deposition [*Sarmiento*, 1993]. Satellite-derived
57 ocean colour data has recently been used to investigate localised increases in PP
58 following volcanic eruptions in Mikakejima, Japan [*Uematsu et al.*, 2004], Montserrat
59 [*Duggen et al.*, 2007], Kasatochi, Alaska [*Langmann et al.*, 2010] and Anatahan,
60 Mariana Islands [*Lin et al.*, 2011].

61 Another unusual event with the potential to alter phytoplankton bloom
62 dynamics in the subpolar North Atlantic also occurred in 2010. The NAO index has
63 been mostly in a positive state since the early 1970s, with occasional negative years
64 (Supplementary Figure S1). However, the winter of 2009/2010 had exceptional NAO
65 conditions, being the second strongest negative NAO on record. Negative NAO
66 conditions are typified by reduced westerly winds and a southward displacement of
67 the North Atlantic storm track. The altered heat fluxes result in a tri-polar structure in

68 sea surface temperature, being warmer in subpolar and subtropical regions and cooler
69 at mid-latitudes (e.g. *Visbeck et al.*, 2003). A rapid wind-driven response in surface
70 currents follows interannual variations in the NAO. In negative NAO periods, the
71 North Atlantic Current shifts eastwards and heat and freshwater transports into the
72 northern North Atlantic increase with the expansion of the subtropical gyre [*Bersch*,
73 2002].

74 The role of the NAO in driving interannual variability in phytoplankton
75 populations has been explored in both the Continuous Plankton Recorder data [*Reid et*
76 *al.*, 1998; *Edwards et al.*, 2001] and in biogeochemical modelling studies [*Henson et*
77 *al.*, 2009; *Patara et al.*, 2011]. The sustained positive NAO period in the 1980's and
78 1990's resulted in reduced phytoplankton populations in both the eastern and western
79 North Atlantic [*Edwards et al.*, 2001]. Correlations at the decadal scale between the
80 NAO and phytoplankton abundance are fairly weak [*Barton et al.*, 2003], however
81 interannual variability in mixing driven by NAO-induced changes in heat and
82 freshwater fluxes are well correlated with phytoplankton bloom timing and magnitude
83 [*Henson et al.*, 2009]. Negative NAO periods typically exhibit a decrease in
84 phytoplankton abundance in the subtropics and an earlier, enhanced bloom in
85 subpolar regions [*Patara et al.*, 2011].

86 We observed a widespread, anomalously strong phytoplankton bloom in
87 satellite ocean colour data throughout the Irminger Basin in the subpolar North
88 Atlantic during spring and summer 2010. The Irminger Basin lies between Greenland
89 and Iceland and is a site of occasional deep convection [*Bacon et al.*, 2003].
90 Phytoplankton dynamics in the basin are typical of the classic North Atlantic spring
91 bloom (*sensu Sverdrup*, 1953), with deep mixed layers in winter ensuring that
92 phytoplankton growth is light limited [*Henson et al.*, 2006a]. The spring bloom is

93 initiated by a shoaling mixed layer associated with a period of net heat flux into the
94 ocean [*Waniek and Holliday, 2006; Henson et al., 2006a*]. Typically, diatoms
95 dominate the initial stages of the bloom, becoming outcompeted by smaller flagellates
96 as silica is depleted [*Henson et al., 2006b; Heath et al., 2008*]. However, unlike most
97 regions of the subpolar North Atlantic, nitrate is not completely depleted during the
98 growing season, with residual concentrations of $\sim 2\text{-}4 \mu\text{mol l}^{-1}$ at the end of summer
99 [*Henson et al., 2003*]. This observation has led to the suggestion that phytoplankton
100 growth is iron limited in summer in the Irminger Basin [*Sanders et al., 2005*]. To
101 directly test this hypothesis, two cruises to the region in spring and summer 2010 were
102 planned as part of the Irminger Basin Iron Study (IBIS) programme. The eruption of
103 the Eyjafjallajökull volcano occurred coincidentally just prior to the first cruise
104 allowing the investigation of the influence of volcanic ash deposition on the
105 biogeochemistry of the region [*Achterberg et al., 2013*].

106 In addition to the two cruises in 2010, the Irminger Basin was also visited in
107 spring and summer 2002, and so here we are able to compare the unusual conditions
108 in 2010 to the more typical conditions observed in 2002. We use a combination of
109 satellite data, *in situ* data and model output to investigate both unusual forcing events
110 – the volcanic eruption and the extreme negative NAO – as possible mechanisms to
111 explain the anomalous bloom.

112

113 **2. Data and Methods**

114 MODIS Aqua Level-3 satellite-derived chlorophyll concentration (chl) data
115 (R2012.0) at 8-day, 9 km resolution for July 2002-December 2010 were obtained
116 from NASA (<http://oceancolor.gsfc.nasa.gov/>). Satellite-derived primary production
117 PP estimates were made using the standard Vertically Generalised Productivity Model

118 [Behrenfeld and Falkowski, 1997]. Volcanic ash carried in the atmosphere can
119 interfere with satellite ocean colour retrievals, resulting in a false increase in chl
120 [Claustre *et al.*, 2002]. To investigate whether airborne ash may have interfered with
121 the satellite chl retrieval, the time series of MODIS Level-3 aerosol optical thickness
122 (AOT) data in the Irminger Basin was examined. This showed only two 8-day
123 periods during which AOT was greater than the range found in previous years (1st-8th
124 May and 18th-25th June; Supplementary Figure S2). The first period occurs during the
125 active eruption phase of the volcano, but the elevated AOT does not coincide with an
126 anomalous increase in chlorophyll (Figure 1b). The second period of unusually high
127 AOT occurs more than one month after the eruption ended, and again does not
128 correspond with anomalously high chl. MODIS Level-3 processing by NASA has a
129 high level of quality control, with 27 flags including those for failed atmospheric
130 correction and failed chlorophyll retrieval. In this case, we conclude that the NASA
131 processing successfully excluded the majority of airborne ash-affected pixels from the
132 Level-3 chl product. *In situ* chl measurements from 2002 and 2010 in the central
133 Irminger Basin (Figure 1c) agree well with the satellite values, giving further
134 confidence that volcanic ash is not unduly impacting the satellite-derived chl data.

135 Monthly wind data for 1998-2010 were obtained from the NCEP/NCAR
136 Reanalysis project [Kalnay *et al.*, 1996]. Monthly optimally interpolated fields of
137 salinity and temperature for 1998-2010 were obtained from the Hadley Centre (EN3
138 dataset derived from a variety of data sources, including Argo floats and the World
139 Ocean Database). Full details of the quality control and data processing can be found
140 in Ingleby and Huddleston [2007]. Density was calculated from temperature and
141 salinity fields using the International Equation of State for Seawater (IES80). Mixed

142 layer depth was estimated from individual Argo float profiles collected in the central
143 Irminger Basin from 2001-2011 using the *Holte and Talley* [2009] density algorithm.

144 Two cruises to the Irminger Basin took place aboard the *RRS Discovery* during
145 (26 April-9 May 2010; D350) and after (4 July-11 August 2010; D354) the
146 Eyjafjallajökull eruption as part of the IBIS programme [*Achterberg et al.*, 2013].
147 Here we compare nutrient and chl concentrations measured on the 2010 cruises to
148 those measured during the UK Marine Productivity programme to the same region in
149 2002 [*Holliday et al.*, 2006]. The 2002 cruises took place during similar periods as in
150 2010 (18 April-27 May 2002; D262 and 25 July-28 August 2002; D264). On all
151 cruises, macronutrients were determined using a Skalar San Plus autoanalyser
152 [*Kirkwood*, 1996] and samples for chl were filtered through 25 mm Whatman GF/F
153 filters, extracted in 90% acetone and determined fluorometrically. Surface chl
154 samples were taken from the ship's continuous thermosalinograph outflow from an
155 intake of 5 m depth. Nutrient data are reported as integrated euphotic zone values,
156 where euphotic depth was estimated from satellite chl using the method of *Morel*
157 [1988]. The temperature and salinity characteristics of the Irminger Basin in 2010 are
158 compared to data collected south of Greenland in 2008 (21 August-25 September
159 2008; D332; *Bacon*, 2010). A map showing all the cruise stations used in this study is
160 presented in Supplementary Figure S3. The 'central Irminger Basin' is defined here
161 as the region bounded by the 1500 m depth contour and north of 58°N, east of 42°W.
162 Results reported for the central Irminger Basin represent a spatial average of all
163 measurements made in this region

164

165 **3. Results**

166 **3.1 Chlorophyll concentration**

167 Satellite-derived chlorophyll images reveal the extent of the anomalous bloom
168 in the Irminger Basin in summer 2010. In early-mid July, the central Irminger Basin
169 experienced unusually high chl concentrations, as revealed in the anomaly map in
170 Figure 1a. The chl concentration in individual pixels was as much as 5 mg m^{-3} greater
171 than the mean of previous years. Examination of the time series of satellite chl data
172 averaged over the central Irminger Basin (Figure 1b), shows that the unusual chl
173 signal in 2010 was a function of the anomalous timing of the bloom peak, in addition
174 to the extended period of high chl concentration, which continued throughout the
175 autumn. The exceptionally high chl concentration in summer 2010 is confirmed by
176 comparison of *in situ* chl samples with the conditions observed in 2002 (Figure 1c).
177 Although spring chl was similar in both years ($0.8\text{-}0.9 \text{ mg m}^{-3}$), chl was significantly
178 higher in summer 2010 (2.2 mg m^{-3}) than in 2002 (0.9 mg m^{-3}). In 2003-2009 and
179 2011, the evolution of chl through the year follows the typical North Atlantic bloom
180 pattern with a rapid increase in chl in late April/early May, followed shortly after by
181 maximum chl values of $\sim 1 \text{ mg m}^{-3}$ in late May/early June. A reduction in chlorophyll
182 during summer is followed by a smaller autumn bloom in late August. In 2010, the
183 bloom progresses in an altogether different manner. The bloom starts as normal in
184 early May, but instead of rapidly reaching a peak before dying back in summer, the
185 chl concentration continues to rise, finally reaching its peak in mid-July, with elevated
186 concentration persisting through autumn 2010. Chlorophyll concentrations then
187 returned to normal levels in 2011. Clearly, the normal seasonal cycle of
188 phytoplankton growth was perturbed in the Irminger Basin in 2010, but was this due
189 to changes in physical forcing or a volcanic fertilisation effect?

190 **3.2 Hydrographic conditions**

191 The NAO in winter 2009/2010 was in an extreme negative phase
192 (Supplementary Figure S1). During negative phases of the NAO, surface pressure
193 increases in the Icelandic low and decreases in the Azores high, resulting in weaker
194 westerly winds and a southward shift of the storm track [Visbeck *et al.*, 2003]. In the
195 case of 2010, the wind during December 2009-June 2010 is either northward (in
196 January and March) or eastward (in February and May), i.e. in the opposite direction
197 entirely, compared to mean conditions. Wind speed is also exceptionally high in May
198 2010 (Figure 2).

199 The hydrographic conditions in the Irminger Basin in 2010 were also
200 anomalous. Transects of density anomaly along 33 °W (Figure 3) show a fresh
201 anomaly intruding into the Irminger Basin from ~ April onwards, inundating the
202 entire basin by August and persisting until December. The anomaly extends over
203 only the top 50-80 m of the water column, i.e. it likely originates from anomalous
204 surface, or near-surface, conditions. Theta-S plots from 2010 provide insight into the
205 likely source of the anomalous water mass in the central Irminger Basin (Figure 4).
206 The theta-S characteristics of the upper ocean in the central Irminger Basin in 2010
207 are very similar to data collected along a transect south of Cape Farewell in early
208 September 2008 [Bacon *et al.*, 2010]. Although the 2010 surface waters are warmer
209 than in 2008, they occupy a theta-S space that is absent in the 2008 data; that is, a
210 mixing region between the typical central Irminger Basin surface layer (salinity of ~
211 34.87-35.05, as in 2008) and the central gyre fresh pool (salinity of ~ 34.65-34.75). A
212 plot of isohalines in the region also demonstrates the anomalous extent of freshwater
213 in the Irminger Basin in 2010 (Figure 5). In March, the location of the isohaline
214 (salinity of 35.02) in 2010, relative to previous years, is unusually far east at 52-54
215 °N. By June 2010 the isohaline is further north and east than is typical at 58-60 °N,

216 indicating a significant change in surface water properties, and by September 2010 the
217 isohaline is north and east of its usual position, indicating anomalously fresh water
218 has inundated a large portion of the Irminger Basin. The unusual hydrographic
219 conditions are also reflected in the mixed layer depth, which remained shallower than
220 normal throughout the autumn (Figure 6).

221 The freshwater intrusion appears to have also introduced anomalous
222 macronutrient conditions, particularly in the southern Irminger Basin. Comparison of
223 nutrient concentrations during the 2010 cruises to similarly timed spring and summer
224 cruises in 2002 suggest that nitrate concentration in spring was similar in the two
225 years, but the summer nitrate was lower in summer 2010 than 2002 (Figure 7). The
226 silica concentration was slightly lower in spring 2010 than in 2002, but similar during
227 the summer cruise (Figure 7). The ratio of N:Si consumed between the spring and
228 summer cruises was 1:1 in 2002, the expected value for a diatom dominated bloom
229 [Brzezinski, 1985], but was 3:1 in 2010.

230 **3.3 Volcanic dust deposition**

231 In addition to the unusual hydrographic conditions observed in 2010, the
232 Eyjafjallajökull volcano in Iceland was actively erupting between 15th April and 23rd
233 May. The ash ejected from the volcano was approximately 7.6 % iron oxide by
234 weight [Achterberg *et al.*, 2013] and so could potentially have added substantial
235 quantities of iron to the surface ocean. Estimates of the iron deposition over the
236 region were made by Achterberg *et al.* [2013] using an atmospheric Lagrangian
237 particle dispersion model for the spatial distribution of ash deposition [Stohl *et al.*,
238 2011] and estimates of ash sinking rates and modelled iron dissolution. A map of iron
239 deposition from the volcanic eruption (Figure 8a) shows that a maximum of ~ 0.08
240 nmol l⁻¹ of iron were likely deposited in the very northern part of the Irminger Basin,

241 and $\sim 0.005 \text{ nmol l}^{-1}$ in the central basin, over the course of the eruption. The time
242 series of iron deposition in this region (Figure 8b) shows that the vast majority was
243 deposited on just one day: 14th May 2010.

244 Chlorophyll concentrations and hydrographic conditions returned to normal in
245 2011, and the NAO index, although still negative, was within the range of previous
246 winter conditions (Figure S1). This implies that the anomalous conditions of 2010
247 resulted from a one-off perturbation to the system, rather than a prolonged regime
248 shift, and that winter mixing in 2010/11 ‘reset’ the system for the following year’s
249 spring bloom.

250

251 **4. Discussion**

252 Satellite-derived chl from the Irminger Basin typically depicts a short, intense
253 bloom in spring, followed by a summer minimum [*Henson et al.*, 2006a]. However,
254 2010 exhibited highly anomalous conditions, with an extended period of high chl
255 persisting from early May through October, with a peak in mid-July. Total annually
256 integrated primary production in the Irminger Basin, estimated from satellite-derived
257 data was $\sim 50\%$ greater in 2010 than the mean of 2003-2009 and 2011, implying
258 potentially significant impacts on CO₂ drawdown and carbon export.

259 The atmospheric conditions in winter 2009/2010 reflect the ‘Warm Arctic-
260 Cold Continents’ climate pattern, which has occurred only 3 times in the last 160
261 years [*Overland et al.*, 2010]. The particularly cold winter in northern Europe and the
262 eastern USA in 2009/2010 was in contrast to exceptionally warm Arctic temperatures,
263 e.g. in Baffin Bay, northeastern Canada, where winter air temperature was $\sim 8 \text{ }^\circ\text{C}$
264 warmer than usual [*Overland et al.*, 2010]. These conditions resulted in increased ice
265 melt over much of the Arctic [*Stroeve et al.*, 2011]. As indicated by the unusual

266 progression of isohalines (Figure 5) and the theta-S characteristics of waters in the
267 southern central Irminger Basin in 2010 (Figure 4), this upper ocean freshwater signal
268 is likely to have originated from south of Cape Farewell where a pool of relatively
269 fresh water typically resides [Reverdin *et al.*, 2002]. The region of the freshwater
270 pool is strongly influenced by the Labrador Current that flows south-eastward,
271 transporting very fresh water from Davis Strait to Newfoundland. Data from
272 Lagrangian drifters has demonstrated that the Labrador and North Atlantic currents
273 intensified under the negative NAO conditions of 1996, although the recirculation in
274 the Irminger Basin weakened [Flatau *et al.*, 2003]. In addition, an increased
275 northward transport of heat and freshwater into the Irminger Basin along the western
276 side of the Mid-Atlantic Ridge was observed [Bersch, 2002]. In 2010, the extreme
277 negative NAO may have resulted in intensification of the Labrador Current and hence
278 freshwater influx to the central subpolar gyre. Anomalous wind conditions in 2010
279 may have then driven the fresh surface waters northeastward, overcapping the central
280 Irminger Basin.

281 The freshwater intrusion may also have altered nutrient conditions in the
282 region, as Labrador Current water has an excess of both phosphate and silicate
283 relative to nitrate [Harrison and Li, 2007] and transports Arctic species of plankton
284 south to the Newfoundland shelf [Head and Pepin, 2010]. The unusual nutrient
285 drawdown ratios shown in Figure 7 arise partly from the lower euphotic zone silica
286 concentrations in spring 2010, relative to nitrate and phosphate, which seems counter
287 to a Labrador Current origin for the freshwater anomaly. Historical macronutrient
288 data extracted from the World Ocean Database for 1980-2004 suggests that silica
289 concentrations in spring 2010 were indeed lower than the mean, suggesting that the
290 diatom bloom had already begun prior to the spring cruise. Silica concentrations in

291 the central Irminger Basin were, in general, around average in summer 2010
292 (Supplementary Figure S4), except along the southern transect (Figure 7f). The
293 anomalously high silica concentrations in the southern Irminger Basin may be a
294 remnant signature of the enhanced nutrient concentrations introduced to the basin with
295 the freshwater anomaly. The anomalous nutrient supply conditions are also reflected
296 in the unusual spring to summer N:Si drawdown ratio, which was 3:1 in 2010 rather
297 than the typical 1:1, suggesting that either the seasonal consumption by phytoplankton
298 of silica relative to nitrate was reduced in 2010 relative to 2002, or that an additional
299 input of silica occurred between May and August, perhaps associated with the
300 freshwater anomaly. This latter hypothesis is consistent with our observation that the
301 spring cruise occurred before the freshwater had fully inundated the basin (Figures 3
302 and 5), but by the time of the summer cruise, the freshwater anomaly had arrived at ~
303 60 °N coinciding with higher than normal silicate concentrations in the southern
304 central Irminger Basin (Figures 5 and 7).

305 A change in the N:Si drawdown ratio may also imply a change in
306 phytoplankton community structure in 2010, from the typical diatom dominated
307 population expected in spring in the Irminger Basin [*Sanders et al.*, 2005] to a
308 phytoplankton population that consumed nitrate in greater quantities than silica. This
309 observation would be consistent with the canonical North Atlantic seasonal
310 succession, where diatoms are succeeded by other phytoplankton functional types as
311 silica becomes depleted. However, silica concentrations were greater than 2 mmol m⁻³
312 ³ in most of the Irminger Basin during the summer cruise, i.e. above the level where
313 diatoms may be out-competed by other species (Brown et al., 2003). Nevertheless,
314 the N:Si drawdown ratio was not 1:1 as expected for diatoms, suggesting that the
315 summer phytoplankton constituted a mixed community. A full taxonomic analysis of

316 the phytoplankton community structure for the 2010 cruises is ongoing, but initial
317 observations confirm the presence of an unusually large proportion of *Coccolithus*
318 *pelagicus* (A. Poulton, pers. comm.), a species abundant in the Labrador Sea [Ziveri *et*
319 *al.*, 2004]. *C. pelagicus* may thus have been advected into the Irminger Basin with the
320 freshwater anomaly and contributed to the unusual nutrient drawdown ratios in 2010.

321 Either the influence of the warmer than usual air temperatures in the region,
322 and/or the freshwater intrusion resulted in an unusually shallow mixed layer depth in
323 autumn 2010. This is likely to have extended the phytoplankton growing season (as
324 seen in the satellite-derived chl data; Figure 1b), which is typically light limited in late
325 autumn and winter [Henson *et al.*, 2006a]. Even if the light conditions were suitable
326 for phytoplankton growth for an extended period of time in 2010, this is unlikely to be
327 the sole reason for the anomalous bloom, as sufficient nutrients would also be
328 required. Although an additional source of nutrients may have been introduced to the
329 region by the unusual hydrographic conditions, it seems unlikely, if not impossible,
330 that this alone could have fuelled the exceptional increase in PP (satellite-derived
331 estimates suggest annually integrated PP was ~ 50% greater in 2010 than the mean).
332 Any additional nitrate introduced to the region would likely need to be supplemented
333 by increased rates of nutrient recycling to sustain these high rates of PP.

334 In situ measurements of ammonium concentration within the mixed layer
335 revealed a 500-fold increase between the spring and summer cruises, confirming that
336 intense recycling was occurring during the summer bloom (E. Achterberg,
337 unpublished data). We have no other ammonium data from this region, and so cannot
338 establish whether the concentrations were unusually high compared to other more
339 typical years. However, atypically for a high latitude, open ocean region, very high
340 ammonium concentrations (up to 2 $\mu\text{mol l}^{-1}$) were observed immediately below the

341 mixed layer in summer. The freshwater cap present in the Irminger Basin in 2010
342 may have allowed retention of the ammonium within the euphotic zone, potentially
343 providing a significant quantity of nitrogen to support the high productivity observed
344 throughout the summer. Our results suggest that the relatively warm spring/summer
345 of 2010, combined with the shallow mixed layer, may have favoured increased rates
346 of nitrogen recycling relative to other years.

347 The anomalous bloom may also have been influenced by reduced grazing
348 pressure. The abundance and behaviour of mesozooplankton in the central Irminger
349 Basin in summer 2010 was comparable to other years, based on measurements of
350 individual body size, gut clearance rates and weight-specific ingestion (S. Giering,
351 unpublished data) However, zooplankton were only grazing ~ 0.5-5 % of PP per day,
352 i.e. top down control of the bloom was very weak. Zooplankton seem to have been
353 unable to increase their grazing rate to respond to the anomalous bloom in 2010, so
354 that, in contrast to normal conditions, PP remained high throughout summer and into
355 autumn. Analysis of a decadal time series of copepods from the Continuous Plankton
356 Recorder survey, suggested that the abundance and population dynamics of *Calanus*
357 *finmarchicus* are insensitive to climate variability in this region [Heath *et al.*, 2008].
358 Our results suggest that the mesozooplankton population was incapable of altering its
359 behaviour in response to variability in conditions, so that grazing rates did not
360 increase despite anomalously high phytoplankton abundance. Although the bloom
361 may not have been under top-down control, maintaining the high phytoplankton
362 biomass through summer and autumn would still have required sufficient additional
363 nutrients.

364 An alternative explanation for the anomalous bloom evolution in 2010 lies
365 with the eruption of the Eyjafjallajökull volcano. Ash deposited onto the sea surface

366 during an eruption will leach iron and other metals into the upper ocean. However,
367 for any additional deposited iron to have a fertilisation effect, phytoplankton growth
368 must be iron limited. Some evidence for iron limitation in this region comes from
369 iron addition experiments conducted in summer 2007 in the Iceland Basin and in
370 summer 2010 in the Irminger Basin, which both demonstrated an increase in chl
371 compared to controls [*Nielsdottir et al.*, 2009; *Ryan-Keogh et al.*, 2013]. Indirect
372 evidence suggesting potential iron limitation in the Irminger Basin also came from the
373 Marine Productivity cruises in 2002. Typically, one would expect that after silica
374 becomes depleted, diatoms would become out-competed by other phytoplankton
375 functional types, which would consume the remaining nitrate. However, *Sanders et*
376 *al.* (2005) established that, although silica is depleted in surface waters in summer,
377 non-limiting concentrations of nitrate remain at the end of the growing season,
378 suggesting that iron limitation of phytoplankton growth may inhibit complete nitrate
379 drawdown in the Iceland, and possibly Irminger, Basins.

380 Results from an atmospheric transport model, combined with estimates of iron
381 content and dissolution rates (see *Achterberg et al.*, 2013 for details), suggest that ash
382 from the eruption may have contributed an additional $\sim 0.005 \text{ nmol l}^{-1}$ of dissolved
383 iron to the central Irminger Basin, the majority of it in one day, 14th May (Figure 8).
384 Elevated chl concentration ($\sim 0.3 \text{ mg m}^{-3}$ higher than the mean) is evident in the
385 Irminger Basin in anomaly maps for the 9th-16th May period (Supplementary Figure
386 S5), but has receded by the following week, when chl is lower than the mean.

387 The relatively transient nature of any stimulation of phytoplankton growth by
388 ash-borne iron was confirmed by shipboard experiments conducted with ash from the
389 Eyjafjallajökull eruption. Bioassays conducted during the summer 2010 cruise found
390 that addition of 9 mg l^{-1} of ash ($\approx 4.6 - 16 \text{ nM DFe}$) to Iceland Basin populations

391 induced an increase in phytoplankton biomass, although the response was weaker than
392 to addition of 2 nM FeCl₃, i.e. much of the dissolved iron released from the ash in
393 seawater was not bioavailable [Achterberg *et al.*, 2013]. The ash also sank rapidly,
394 with settling experiments suggesting that the particles fell through the upper mixed
395 layer (~ 30 m deep in spring) in ~ 90 minutes, during which time all the salts leached
396 from the particles [Achterberg *et al.*, 2013]. This is even faster than the previously
397 reported residence time of atmospheric iron inputs in the surface ocean of 2-7 weeks
398 [Sarhou *et al.*, 2003]. These results are consistent with the observation during the
399 summer 2010 (i.e. post-eruption) cruise of a lack of elevated surface iron
400 concentrations in the region offshore of Eyjafjallajökull [Achterberg *et al.*, 2013].
401 Taken together these observations imply that any fertilisation effect due to ash
402 deposition was short-lived.

403

404 **5. Conclusion**

405 A highly anomalous chlorophyll bloom occurred in the central Irminger Basin
406 in 2010, persisting throughout the summer and autumn. We present here several
407 observations of unusual conditions in 2010 that may have influenced the development
408 of the anomalous phytoplankton bloom:

409 • The North Atlantic Oscillation was in an extreme negative phase in winter
410 2009/10; the second most negative on record since winter 1968/69 (Supplementary
411 Figure S1).

412 • Wind direction was reversed in spring 2010 compared to normal conditions,
413 coming from the south or east (Figure 2).

414 • A surface freshwater anomaly was observed extending throughout the central
415 Irminger Basin in summer 2010 to a depth of ~ 30 m (Figure 3).

416 • The freshwater anomaly had characteristics similar to that of the central gyre
417 fresh pool, situated south of Cape Farewell (Figure 4), and migrated northeastwards
418 into the Irminger Basin during summer 2010 (Figure 5).

419 • The mixed layer shoaled earlier than usual and stayed relatively shallow
420 through autumn (Figure 6).

421 • The central Irminger Basin phytoplankton community composition had an
422 unusually large proportion of *Coccolithicus pelagicus*, usually abundant in the
423 Labrador Sea.

424 • Nutrient utilisation was anomalous, with N:Si drawdown ratios of 3:1, rather
425 than the usual 1:1 (Figure 7).

426 • Zooplankton grazing rates did not increase in tandem with PP during the
427 summer.

428 • The Eyjafjallajökull volcano erupted in April/May 2010 depositing ash in the
429 northern Irminger Basin, which may have added a total of $\sim 0.005\text{-}0.08 \text{ nmol l}^{-1}$ of
430 iron to the region (Figure 8).

431 Although we can provide no definitive answer to what caused the anomalous bloom,
432 the balance of evidence points to the unusual hydrographic conditions of 2010, with
433 the volcanic eruption playing a relatively minor role.

434 Ongoing analysis of the cruise data collected as part of the IBIS programme
435 may reveal some additional clues to the causes, and importantly, consequences of the
436 anomalous bloom. A key question is whether the bloom resulted in an increase in
437 organic carbon export, and therefore may have had a significant impact on the
438 biogeochemistry of the region. Introduction of iron to the surface ocean via
439 deposition of volcanic ash has been postulated as a driver of reductions in atmospheric
440 CO_2 [Watson *et al.*, 1997], due to the stimulation of additional carbon export. In the

441 case of the Eyjafjallajökull eruption and the Irminger Basin, the volcanic eruption
442 seems to have had a fairly minor effect. A volcanic eruption would need to produce
443 substantially more ash, over a longer period, with direct deposition over a high
444 nutrient-low chlorophyll area in order to affect atmospheric CO₂ concentrations.

445

446 **Acknowledgements**

447 Many thanks to the captain, crew and scientific parties of the IBIS cruises, particularly
448 the principal scientists Mark Moore and Eric Achterberg (University of
449 Southampton). The cruises were supported by the Natural Environment Research
450 Council (UK) through grant NE/E006833/1. The dispersion modelling results were
451 kindly provided by Andreas Stohl and Sabine Eckhardt (Norsk Institut for
452 Luftforskning). SeaWiFS data were provided by GSFC/NASA in accordance with the
453 SeaWiFS Research Data Use Terms and Conditions Agreement. NCEP Reanalysis
454 data provided by the NOAA/OAR/ESRL PSD, Boulder, Colorado, USA, from their
455 Web site at <http://www.esrl.noaa.gov/psd/>. Argo float data were collected and made
456 freely available by the International Argo Project and the national programmes that
457 contribute to it (<http://www.argo.net>). This work was supported by NERC grant
458 NE/G013055/1 to SAH.

459

460 **References**

461 Achterberg, E. P., C. M. Moore, S. A. Henson, S. Steigenberger, A. Stohl, S.
462 Eckhardt, L. C. Avendano, M. Cassidy, D. Hembury, J. K. Klar, M. I. Lucas, A. I.
463 Macey, C. M. Marsay, and T. J. Ryan-Keogh (2013), Natural iron fertilisation by the
464 Eyjafjallajökull volcanic eruption, *Geophys. Res. Lett.*, doi: 10.1002/grl.50221.

465 Bacon, S., W. J. Gould, and Y. L. Jia (2003), Open-ocean convection in the Irminger
466 Sea, *Geophys. Res. Lett.*, 30(5), 1246, doi:10.1029/2002gl016271.

467 Bacon, S. (2010), RSS Discovery Cruise 332, 21 Aug – 25 Sep 2008, Arctic Gateway
468 (WOCE AR7). National Oceanography Centre Southampton Cruise Report, 53.

469 Barton, A. D., C. H. Greene, B. C. Monger, and A. J. Pershing (2003), The
470 Continuous Plankton Recorder survey and the North Atlantic Oscillation: Interannual-
471 to multidecadal-scale patterns of phytoplankton variability in the North Atlantic
472 Ocean, *Prog. Oceanogr.*, 58, 337-358.

473 Behrenfeld, M. J., and P. G. Falkowski (1997), Photosynthetic rates derived from
474 satellite-based chlorophyll concentration, *Limnol. Oceanogr.*, 42(1), 1-20.

475 Bersch, M. (2002), North Atlantic Oscillation–induced changes of the upper layer
476 circulation in the northern North Atlantic Ocean, *J. Geophys. Res.*, 107,
477 doi: 10.1029/2001JC000901.

478 Box, J. E., J. Cappelen, D. Decker, X. Fettweis, T. Mote, M. Tedesco, and R. S. W.
479 van de Wal (2010), Greenland, in Arctic Report Card 2010, NOAA.

480 Brzezinski, M. A. (1985), The Si-C-N ratio of marine diatoms - interspecific
481 variability and the effect of some environmental variables, *J. Phycology*, 21(3), 347-
482 357.

483 Claustre, H., A. Morel, S. B. Hooker, M. Babin, D. Antoine, K. Oubelkheir, A.
484 Bricaud, K. Leblanc, B. Queguiner, and S. Maritorena (2002), Is desert dust making
485 oligotrophic waters greener?, *Geophys. Res. Lett.*, 29(10), 1469,
486 doi:10.1029/2001gl014056.

487 Duggen, S., P. Croot, U. Schacht, and L. Hoffmann (2007), Subduction zone volcanic
488 ash can fertilize the surface ocean and stimulate phytoplankton growth: Evidence

489 from biogeochemical experiments and satellite data, *Geophys. Res. Lett.*, 34(1),
490 L01612, doi:10.1029/2006gl027522.

491 Duggen, S., N. Olgun, P. Croot, L. Hoffmann, H. Dietze, P. Delmelle, and C. Teshner
492 (2010), The role of airborne volcanic ash for the surface ocean biogeochemical iron-
493 cycle: a review, *Biogeosciences* 7, 827-844, doi:10.5194/bg-7-827-2010.

494 Edwards, M., P. Reid, and B. Planque (2001), Long-term and regional variability of
495 phytoplankton biomass in the Northeast Atlantic (1960-1995), *ICES J. Mar. Sci.*,
496 58(1), 39-49, doi:10.1006/jmsc.2000.0987.

497 Flatau, M. K., L. Talley, and P. P. Niiler (2003), The North Atlantic Oscillation,
498 surface current velocities, and SST changes in the subpolar North Atlantic, *J. Clim.*,
499 16(14), 2355-2369, doi:10.1175/2787.1.

500 Gudmundsson, M.T., T. Thordarson, A. Höskuldsson, G. Larsen, H. Björnsson, F.J.
501 Prata, B. Oddsson, E. Magnússon, T. Högnadóttir, G.N. Petersen, C.L. Hayward, J.A.
502 Stevenson and I. Jonsdóttir (2012), Ash generation and distribution from the April-
503 May 2010 eruption of Eyjafjallajökull, Iceland, *Nature Scientific Reports*, 2(572), doi:
504 10.1038/srep00572.

505 Harrison, W. G., and W. K. W. Li (2007), Phytoplankton growth and regulation in the
506 Labrador Sea: Light and nutrient limitation, *J. Northw. Atl. Fish. Sci.*, 39, 71-82.

507 Head, E. J. H., and Pepin, P. (2010), Spatial and inter-decadal variability in plankton
508 abundance and composition in the Northwest Atlantic (1958-2006), *J. Plank. Res.*,
509 32(12), 1633-1648, doi:10.1093/plankt/fbq090.

510 Heath, M. R., J. Rasmussen, Y. Ahmed, J. Allen, C. I. H. Anderson, A. S. Brierley, L.
511 Brown, A. Bunker, K. Cook, R. Davidson, S. Fielding, W. S. C. Gurney, R. Harris, S.
512 Hay, S. Henson, A. G. Hirst, N. P. Holliday, A. Ingvarsdóttir, X. Irigoien, P.
513 Lindeque, D. J. Mayor, D. Montagnes, C. Moffat, R. Pollard, S. Richards, R. A.

514 Saunders, J. Sidey, G. Smerdon, D. Speirs, P. Walsham, J. Waniek, L. Webster, and
515 D. Wilson (2008), Spatial demography of *Calanus finmarchicus* in the Irminger Sea,
516 *Prog. Oceanogr.*, 76(1), 39-88, doi:10.1016/j.pocean.2007.10.001.

517 Henson, S. A., R. Sanders, J. T. Allen, I. S. Robinson, and L. Brown (2003), Seasonal
518 constraints on the estimation of new production from space using temperature-nitrate
519 relationships, *Geophys. Res. Lett.*, 30(17), 1912, doi:10.1029/2003gl017982.

520 Henson, S. A., I. Robinson, J. T. Allen, and J. J. Waniek (2006a), Effect of
521 meteorological conditions on interannual variability in timing and magnitude of the
522 spring bloom in the Irminger Basin, North Atlantic, *Deep-Sea Res. I*, 53(10), 1601-
523 1615, doi:10.1016/j.dsr.2006.07.009.

524 Henson, S. A., R. Sanders, C. Hopleton, and J. T. Allen (2006b), Timing of nutrient
525 depletion, diatom dominance and a lower-boundary estimate of export production for
526 Irminger Basin, North Atlantic, *Mar. Ecol. Prog. Ser.*, 313, 73-84,
527 doi:10.3354/meps313073.

528 Henson, S. A., J. P. Dunne, and J. L. Sarmiento (2009), Decadal variability in North
529 Atlantic phytoplankton blooms, *J. Geophys. Res.*, 114, C04013,
530 doi:10.1029/2008jc005139.

531 Holliday, N. P., A. Meyer, S. Bacon, S. G. Alderson, and B. de Cuevas (2007),
532 Retroflection of part of the east Greenland current at Cape Farewell, *Geophys. Res.*
533 *Lett.*, 34(7), L07609, doi:10.1029/2006gl029085.

534 Holliday, N.P., J.J. Waniek, R. Davidson, D. Wilson, L. Brown, R. Sanders, R.T.
535 Pollard, and J.T. Allen (2006), Large-scale physical controls on phytoplankton growth
536 in the Irminger Sea Part I: Hydrographic zones, mixing and stratification, *J. Mar. Sys.*
537 59, 201-218.

538 Holte, J., and L. Talley (2009), A new algorithm for finding mixed layer depths with
539 applications to Argo data and Subantarctic Mode Water formation, *J. Atmos. Ocean.*
540 *Tech.*, 26(9), 1920-1939, doi:10.1175/2009jtecho543.1.

541 Ingleby, B., and M. Huddleston (2007), Quality control of ocean temperature and
542 salinity profiles - historical and real-time data. *J. Mar. Sys.*, 65, 158-175,
543 doi:10.1016/j.jmarsys.2005.11.019.

544 Kalnay, E., M. Kanamitsu, R. Kistler, W. Collins, D. Deaven, L. Gandin, M. Iredell,
545 S. Saha, G. White, J. Woollen, Y. Zhu, M. Chelliah, W. Ebisuzaki, W. Higgins, J.
546 Janowiak, K. C. Mo, C. Ropelewski, J. Wang, A. Leetmaa, R. Reynolds, R. Jenne, D.
547 Joseph (1996), The NCEP/NCAR 40-year reanalysis project, *Bull. Am. Met. Soc.*,
548 77(3), 437-471.

549 Karlsdóttir, S., Á. G. Gylfason, Á. Höskuldsson, B. Brandsdóttir, E. Ilyinskaya, M. T.
550 Gudmundsson, and Þ. Högnadóttir (2012), The 2010 Eyjafjallajökull eruption,
551 Iceland, ICAO report, Ed. B. Þorkelsson.

552 Kirkwood, D.S. (1996), Nutrients: Practical notes on their determination in seawater,
553 ICES Techniques in Marine Environmental Sciences Report 17. Copenhagen,
554 International Council for the Exploration of the Seas.

555 Langmann, B., K. Zaksek, M. Hort, and S. Duggen (2010), Volcanic ash as fertiliser
556 for the surface ocean, *Atmos. Chem. Phys.*, 10(8), 3891-3899.

557 Lin, II, C. M. Hu, Y. H. Li, T. Y. Ho, T. P. Fischer, G. T. F. Wong, J. F. Wu, C. W.
558 Huang, D. A. Chu, D. S. Ko, and J. P. Chen (2011), Fertilization potential of volcanic
559 dust in the low-nutrient low-chlorophyll western North Pacific subtropical gyre:
560 Satellite evidence and laboratory study, *Global Biogeochem. Cycles*, 25, GB1006,
561 doi:10.1029/2009gb003758.

562 Morel, A. (1988), Optical modeling of the upper ocean in relation to its biogenous
563 matter content (Case-I waters), *J. Geophys. Res.*, 93(C9), 10749-10768,
564 doi:10.1029/JC093iC09p10749.

565 Nielsdottir, M. C., C. M. Moore, R. Sanders, D. J. Hinz, and E. P. Achterberg (2009),
566 Iron limitation of the postbloom phytoplankton communities in the Iceland Basin,
567 *Global Biogeochem. Cycles*, 23, GB3001, doi:10.1029/2008gb003410.

568 Overland, J., M. Wang, and J. Walsh (2010), Atmosphere, in Arctic Report Card
569 2010, NOAA.

570 Patara, L., M. Visbeck, S. Masina, G. Krahnemann, and M. Vichi (2011), Marine
571 biogeochemical responses to the North Atlantic Oscillation in a coupled climate
572 model, *J. Geophys. Res.*, 116, C07023, doi:10.1029/2010jc006785.

573 Reid, P. C., B. Planque, and M. Edwards (1998), Is observed variability in the long-
574 term results of the Continuous Plankton Recorder survey a response to climate
575 change?, *Fisheries Oceanogr.*, 7(3-4), 282-288, doi:10.1046/j.1365-
576 2419.1998.00073.x.

577 Reverdin, G., F. Durand, J. Mortensen, F. Schott, H. Valdimarsson, and W. Zenk
578 (2002), Recent changes in the surface salinity of the North Atlantic subpolar gyre, *J.*
579 *Geophys. Res.*, 107, C12, 8010, doi:10.1029/2001JC001010.

580 Robock, A. (2000), Volcanic eruptions and climate, *Rev. Geophys.*, 38(2), 191-219,
581 doi:10.1029/1998rg000054.

582 Ryan-Keogh, T. J., A. I. Macey, M. C. Nielsdóttir, M. I. Lucas, M. C. Stinchcombe,
583 E. P. Achterberg, T. S. Bibby, and C. M. Moore (2013), Spatial and temporal
584 development of phytoplankton iron stress in relation to bloom dynamics in the high
585 latitude North Atlantic Ocean, *Limnol. Oceanogr.*, 58, 533-545.

586 Sanders, R., L. Brown, S. Henson, and M. Lucas (2005), New production in the
587 Irminger Basin during 2002, *J. Mar. Sys.*, 55(3-4), 291-310,
588 doi:10.1016/j.jmarsys.2004.09.002.

589 Sarmiento, J. L. (1993), Carbon-cycle - Atmospheric CO₂ stalled, *Nature*, 365(6448),
590 697-698, doi:10.1038/365697a0.

591 Sarthou, G., A. R. Baker, S. Blain, E. P. Achterberg, M. Boye, A. R. Bowie, P. Croot,
592 P. Laan, H. J. W. de Baar, T. D. Jickells, and P. J. Worsfold (2003), Atmospheric iron
593 deposition and sea-surface dissolved iron concentrations in the eastern Atlantic
594 Ocean, *Deep-Sea Res. I*, 50(10-11), 1339-1352, doi:10.1016/s0967-0637(03)00126-2.

595 Stohl, A., A. J. Prata, S. Eckhardt, L. Clarisse, A. Durant, S. Henne, N. I. Kristiansen,
596 A. Minikin, U. Schumann, P. Seibert, K. Stebel, H. E. Thomas, T. Thorsteinsson, K.
597 Torseth, and B. Weinzierl (2011), Determination of time- and height-resolved
598 volcanic ash emissions and their use for quantitative ash dispersion modeling: the
599 2010 Eyjafjallajokull eruption, *Atmos. Chem. Phys.*, 11(9), 4333-4351,
600 doi:10.5194/acp-11-4333-2011.

601 Stroeve, J. C., J. Maslanik, M. C. Serreze, I. Rigor, W. Meier, and C. Fowler (2011),
602 Sea ice response to an extreme negative phase of the Arctic Oscillation during winter
603 2009/2010, *Geophys. Res. Lett.*, 38, L02502, doi:10.1029/2010gl045662.

604 Sverdrup, H. U. (1953), On conditions for the vernal blooming of phytoplankton, *J.*
605 *Cons. Perm. Int. Explor. Mer*, 18, 287-295.

606 Uematsu, M., M. Toratani, M. Kajino, Y. Narita, Y. Senga, and T. Kimoto (2004),
607 Enhancement of primary productivity in the western North Pacific caused by the
608 eruption of the Miyake-jima Volcano, *Geophys. Res. Lett.*, 31(6), L06106,
609 doi:10.1029/2003gl018790.

610 Visbeck, M., E. P. Chassignet, R. G. Curry, T. L. Delworth, R. R. Dickson, and G.
611 Krahnmann (2003), The ocean's response to North Atlantic Oscillation variability, in
612 *The North Atlantic Oscillation: Climatic Significance and Environmental Impact*,
613 Geophys. Monogr. Ser., vol. 134, Ed. J. W. Hurrell, pp 113-146, AGU, Washington.
614 Waniek, J. J., and N. P. Holliday (2006), Large-scale physical controls on
615 phytoplankton growth in the Irminger Sea, Part II: Model study of the physical and
616 meteorological preconditioning, *J. Mar. Sys.*, 59(3-4), 219-237,
617 doi:10.1016/j.jmarsys.2005.10.005.
618 Watson, A. J. (1997), Volcanic iron, CO₂, ocean productivity and climate, *Nature*,
619 385(6617), 587-588, doi:10.1038/385587b0.
620 Ziveri, P., K. H. Baumann, B. Böckel, J. Bollmann, and J. R. Young (2004),
621 Biogeography of selected Holocene coccoliths in the Atlantic Ocean, p. 403-428. *In*
622 H. R. Thierstein & J. R. Young [eds.], *Coccolithophores. From Molecular Processes*
623 *to Global Impact*. Springer.
624

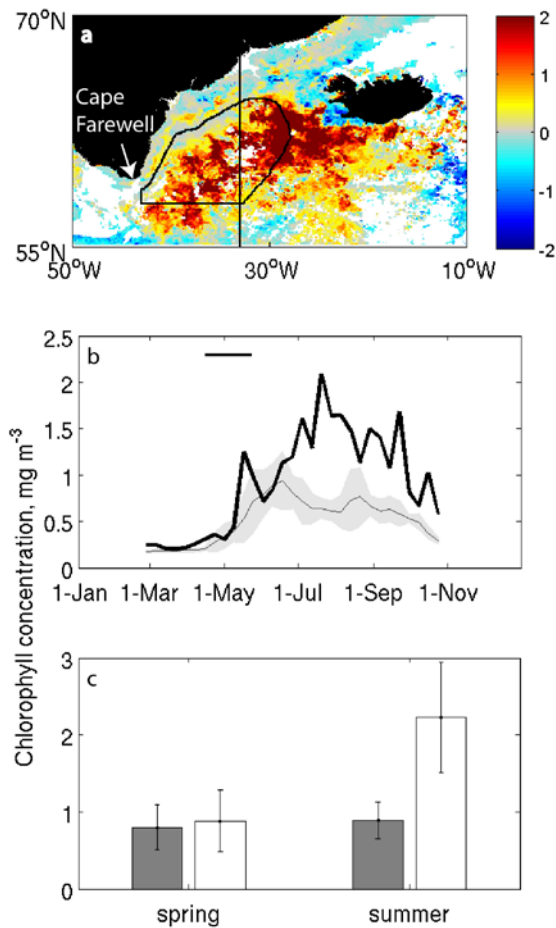


Figure 1: Anomalous chlorophyll conditions in the Irminger Basin in 2010. a) Chlorophyll anomaly (mg m^{-3}) for 12th-19th July 2010, relative to the mean of the same period in 2003-2009 and 2011. The region denoted in this study as the ‘central Irminger Basin’ is outlined in black. The position of the transect plotted in Figure 3 is marked with a vertical black line. b) Satellite-derived time series of chlorophyll concentration in the central Irminger Basin in 2010 (thick black line), the mean (thin grey line) and standard deviation (grey shading) of years 2003-2009 and 2011. Black horizontal line marks the period of the volcanic eruption. c) *In situ* measured chlorophyll concentration (collected from the underway system at ~ 5 m depth) in the central Irminger Basin collected on cruises in spring and summer 2002 (grey bars) and 2010 (white bars). Error bars denote the spatial variability of data within the basin (standard deviation).

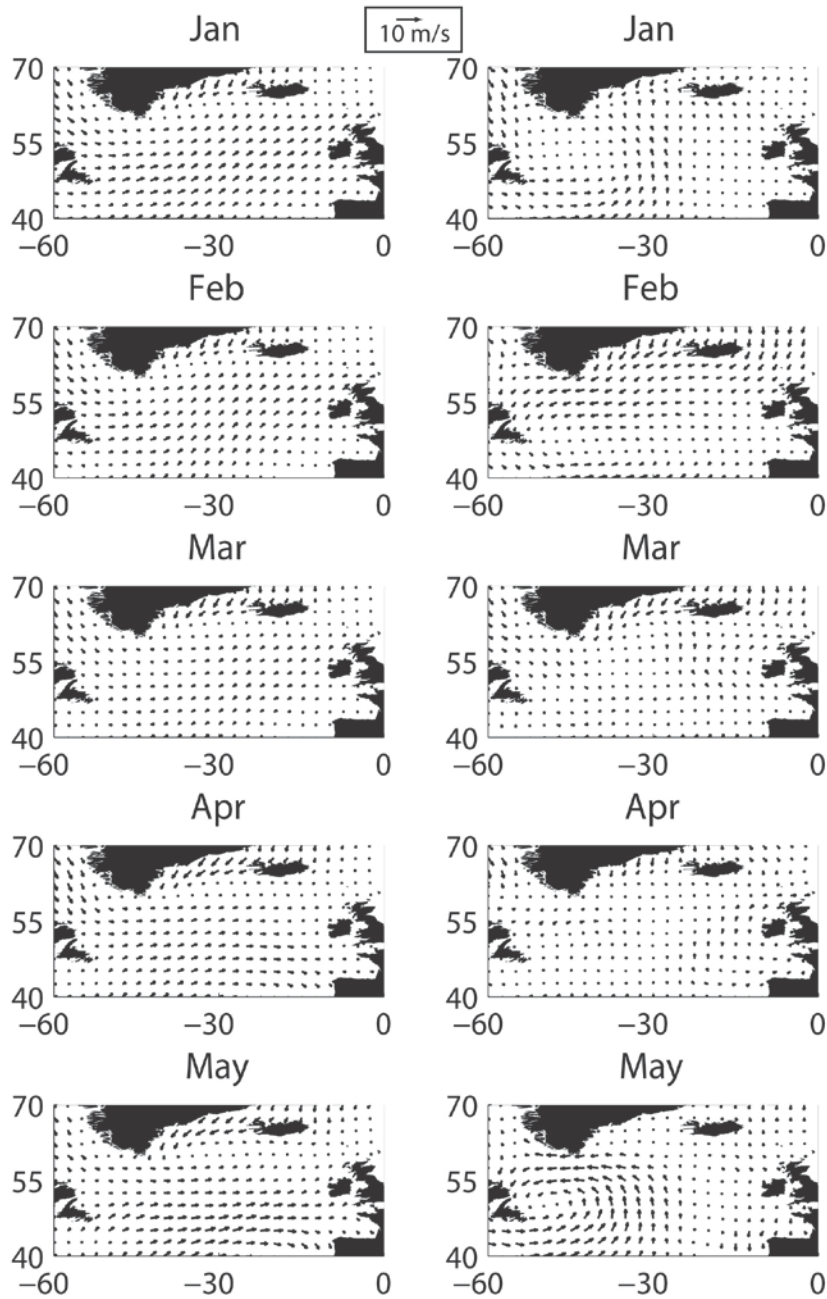


Figure 2: Left column: Mean (1998-2009) wind speed over the North Atlantic in selected months (at 10 m above sea level). Right column: Wind speed in selected months of 2010. Note that the wind direction in February 2010 is reversed with respect to the mean, and that northward wind speeds in May 2010 are anomalously strong.

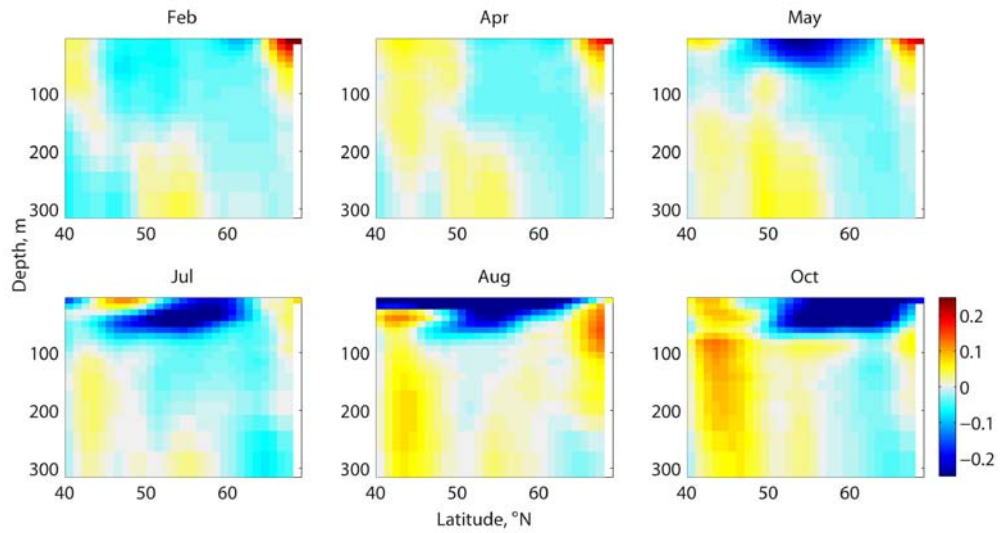


Figure 3: Density anomaly (kg m^{-3}) from the Hadley Centre EN3 dataset for selected months in 2010, relative to the mean of 1998-2009, along a transect at 33 °W.

Note the presence of an anomalously light, fresh water mass entering the Irminger Basin during May, capping the entire region by August and persisting until October.

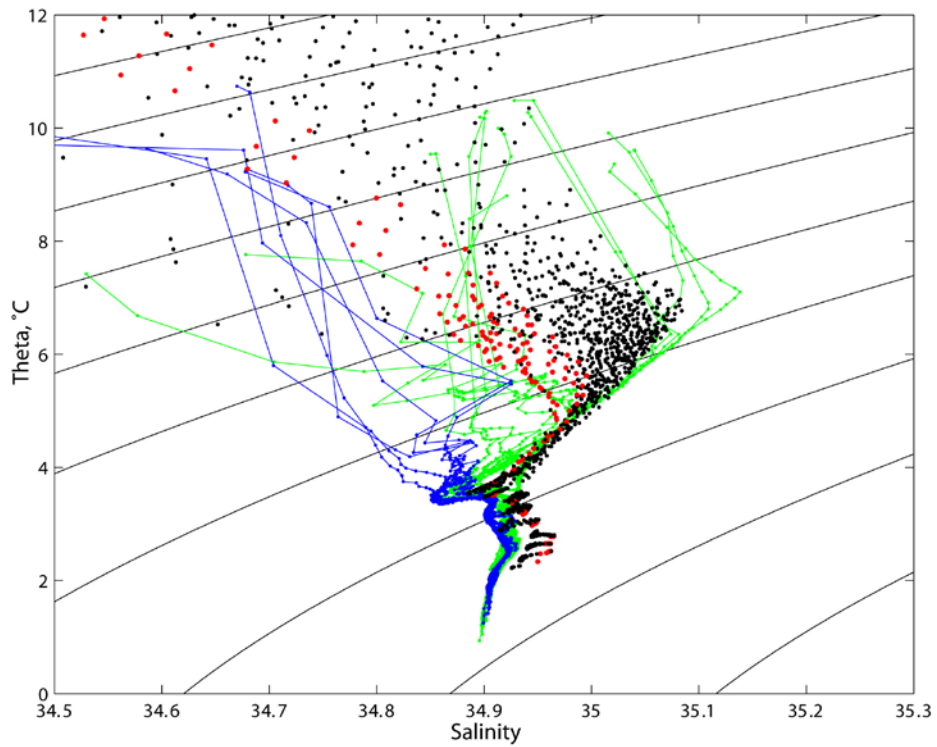


Figure 4: Theta-S plot showing data from early September 2008 along a transect south of Cape Farewell (blue lines) and in the southern Irminger Basin along 59 °N (green lines). Also plotted are data from August 2010 in the central (black dots) and southern (55-56 °N) Irminger Basin (red dots).

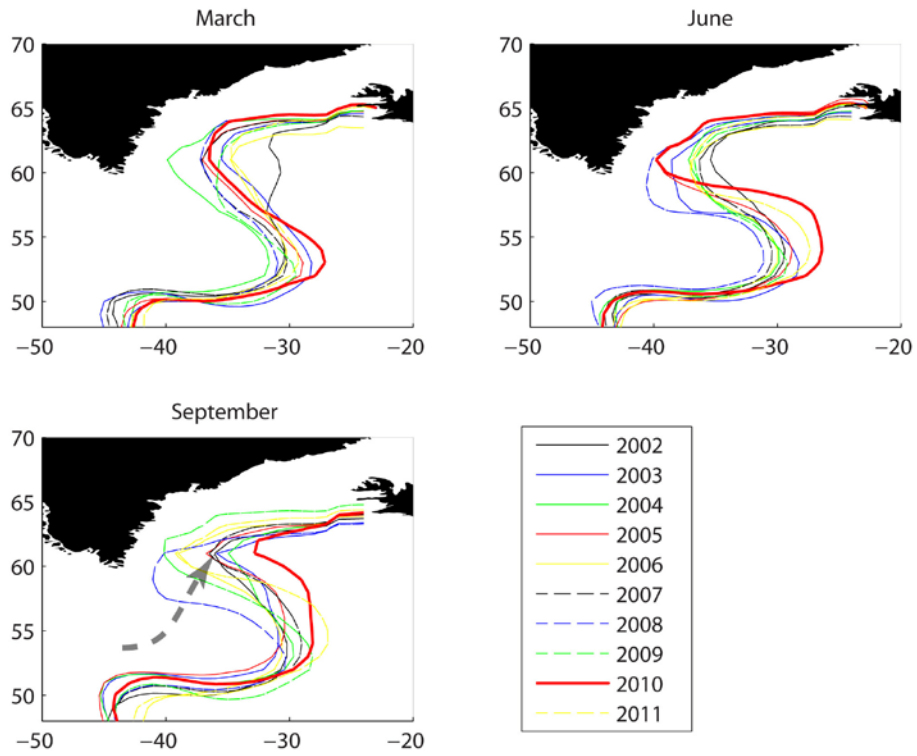


Figure 5: Position of isohalines (salinity = 35.02) in March, June and September for years 2002-2011. The position of the isohaline in 2010 is marked with a thick red line. Note that in 2010 the appearance of the freshwater anomaly perturbs the isohaline to the northeast, suggesting the water mass originated to the southwest. Dashed grey arrow in last panel is a sketch of the hypothesised path of the freshwater intrusion.

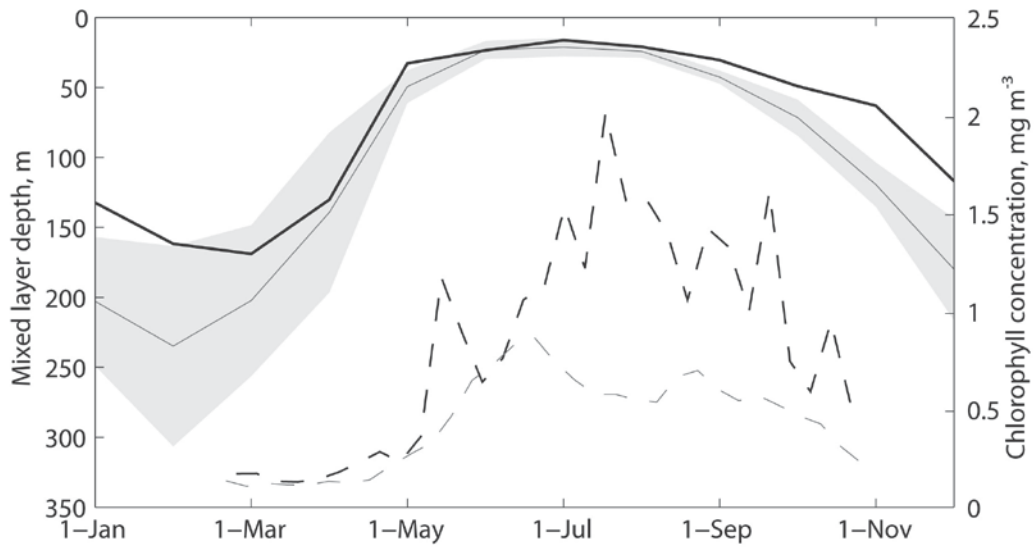


Figure 6: Monthly mixed layer depth in the central Irminger Basin in 2010 (thick black line), the mean (thin grey line) and standard deviation (grey shading) of years 2001-2009 and 2011. Note that the mixed layer in 2010 is shallower than the mean in winter and throughout autumn. Also plotted are chlorophyll concentration in 2010 (black dashed line) and the mean of 2003-2009 and 2011 (grey dashed line) taken from Figure 1b.

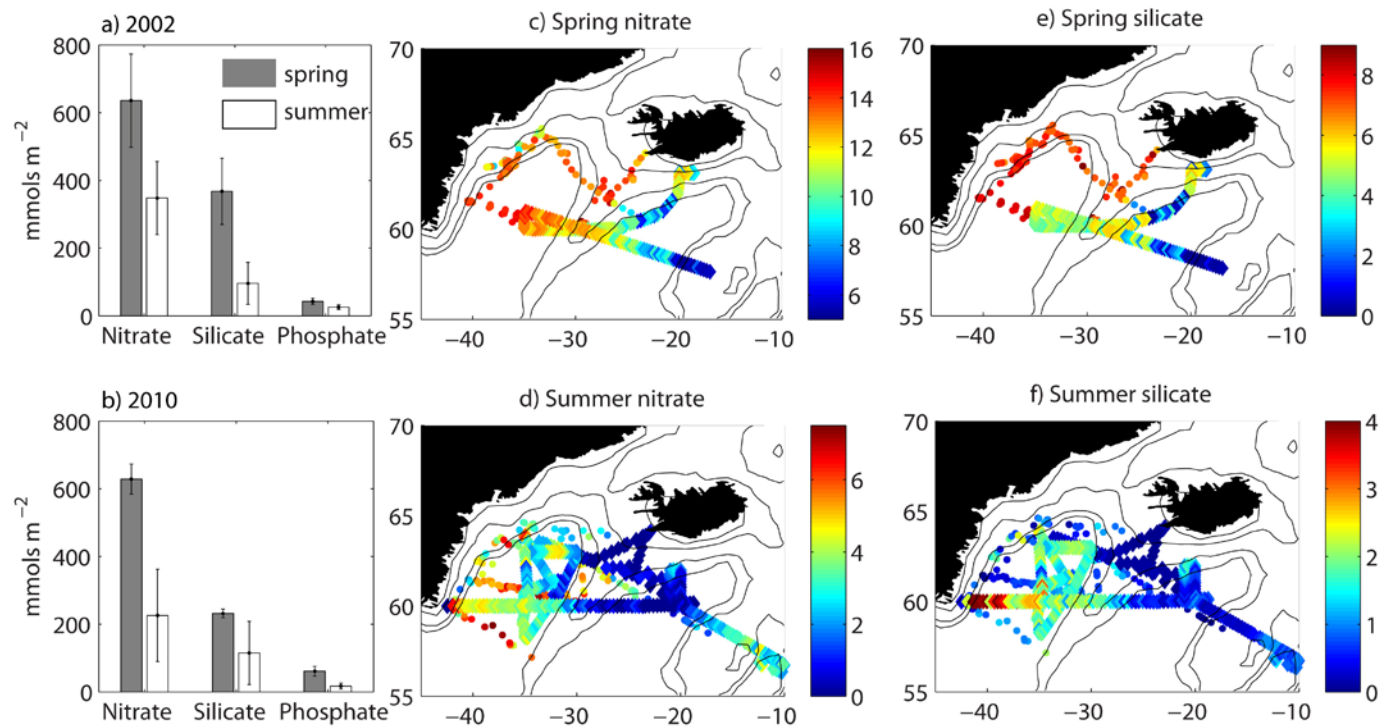


Figure 7: Comparison between integrated euphotic depth macronutrients in the central Irminger Basin in a) 2002 and b) 2010 from cruises in spring (gray bars) and summer (white bars). Error bars denote the spatial variability of data within the basin (standard deviation). c) Nitrate and d) silicate concentrations (mmol m^{-3}) collected underway at ~ 5 m depth on cruises in spring 2002 (small dots) and 2010 (diamonds), and similarly in summer for e) nitrate and f) silicate.

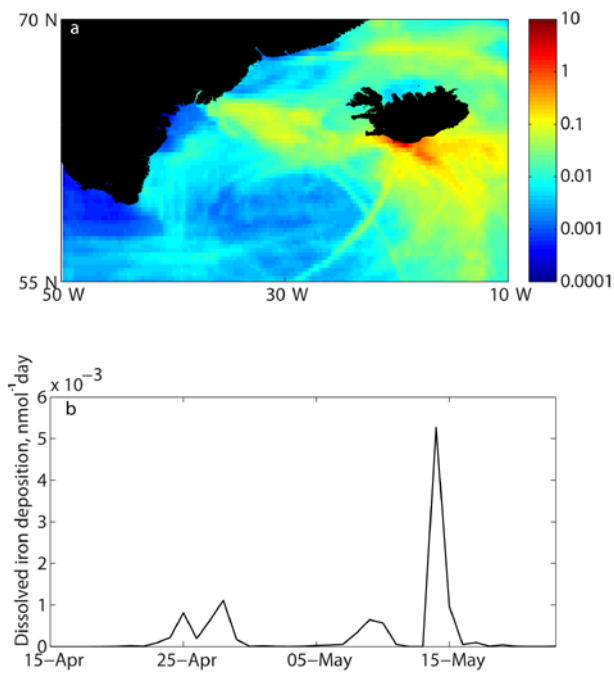


Figure 8: a) Modelled dissolved iron deposition (nmol l^{-1}) from the eruption of the Eyjafjallajökull volcano (April 15-May 23, 2010). For details of the model and estimation of iron deposition see Stohl et al. (2011) and Achterberg et al. (2013). b) Daily modelled iron deposition rates ($\text{nmol l}^{-1} \text{ day}^{-1}$) in the central Irminger Basin during the volcanic eruption.